Journal of Applied Polymer Science

Simultaneous improvement in strength, toughness, and thermal stability of epoxy/halloysite nanotubes composites by interfacial modification

Pan Sun,[1] Guoming Liu,[1] Dong Lv,[2] Xia Dong,[1] Jingshen Wu,[2] Dujin Wang[1]

[1]Beijing National Laboratory for Molecular Sciences, CAS Key Laboratory of Engineering Plastics, Institute of Chemistry, The Chinese Academy of Sciences, Beijing 100190, China

[2]Department of Mechanical and Aerospace Engineering, The Hong Kong University of Science and Technology, Hong Kong, China

Correspondence to: G. Liu (E-mail: gmliu@iccas.ac.cn)

ABSTRACT: This work investigated the effect of silane modification of halloysite nanotubes (HNTs) on the mechanical properties of epoxy/HNTs nanocomposites. Three kinds of silane coupling agents, including 3-(2-aminoethyl)-aminopropyltrimethoxysilane (AEAPS), (3-glycidyloxypropyl)-trimethoxysilane (GPTMS), and octyltriethoxysilane (OTES), were employed. It was shown that the modified HNTs exhibited a better dispersion in the epoxy matrix compared with pristine one. Because of strong interfacial interaction between AEAPS modified HNTs and the epoxy matrix, the nanocomposites exhibited the highest glass transition temperature and modulus among all the samples. On the other hand, AEAPS and GPTMS modified HNTs/epoxy nanocomposites showed enhanced tensile strength and toughness. The toughing mechanisms were identified by the SEM micrographs of the fracture surfaces of the different kinds of samples. In this study, simultaneous enhancement of strength, toughness, and thermal stability of epoxy by the modified HNTs provides a novel approach to produce high-performance thermosets. © 2015 Wiley Periodicals, Inc. J. Appl. Polym. Sci. **2016**, *133*, 43249.

KEYWORDS: composites; graphene and fullerenes; mechanical properties; nanotubes; thermosets

Received 24 August 2015; accepted 19 November 2015

DOI: 10.1002/app.43249

INTRODUCTION

Naturally occurring halloysite nanotubes (HNTs) have attracted extensive attention because of their low cost, immense reserve, excellent thermal, mechanical, and biological properties. Recently, HNTs have been successfully used as nanofillers for reinforcing polymers.[1–5] According to previous studies,[6–9] HNTs could generate comparable mechanical improvement as montmorillonite (MMT) or carbon nanotubes (CNTs) with simple fabricating process. However, 5–10 μm HNTs aggregates are hardly avoided through conventional mixing methods, even in polar polymers.[10] Surface modification is usually carried out to avoid aggregation and further improve the interfacial interaction between HNTs and polymer matrix. In other works, modified HNTs have been successfully incorporated into polypropylene (PP),[2,11] unsaturated polyester (UPE),[12] polyamide (PA),[13,14] and ethylene-propylene-diene monomer rubber (EPDM).[15]

Epoxy resins are types of widely used thermosetting polymers because of their high strength and stiffness, excellent chemical and thermal resistance, ease of processing. However, the intrinsic brittleness of most epoxies restricts their applications. Inorganic nanofillers are often employed to improve the toughness of epoxy resin since these fillers can increase the toughness without sacrificing its rigidity and thermal properties compared with rubber.[16] Among the inorganic rigid nanofillers, HNTs become a promising candidate for toughening epoxy in the last decade. The impact strength and fracture toughness of HNTs-based epoxy nanocomposites have gained different levels of improvement,[17–20] while the tensile strength kept almost unvaried[6,21] or became worse[22] than the neat epoxy. The strain at break decreased with increasing HNTs loading.[6,22] This limited reinforcement might be related to the aggregation of HNTs,[6] which leads to premature failure during deformation.

In literature, chemical treatment of HNTs has been utilized to eliminate aggregation in epoxy resins. Commonly used intercalated agents such as phenylphosphonic acid (PPA)[23,24] and potassium acetate (PA)[21] could reduce the cluster size with the help of ball mill homogenization. On the other hand, surfactants such as cetyltrimethyl ammonium chloride (CTAC) unfavorably led to more HNTs aggregation.[21] The fracture toughness

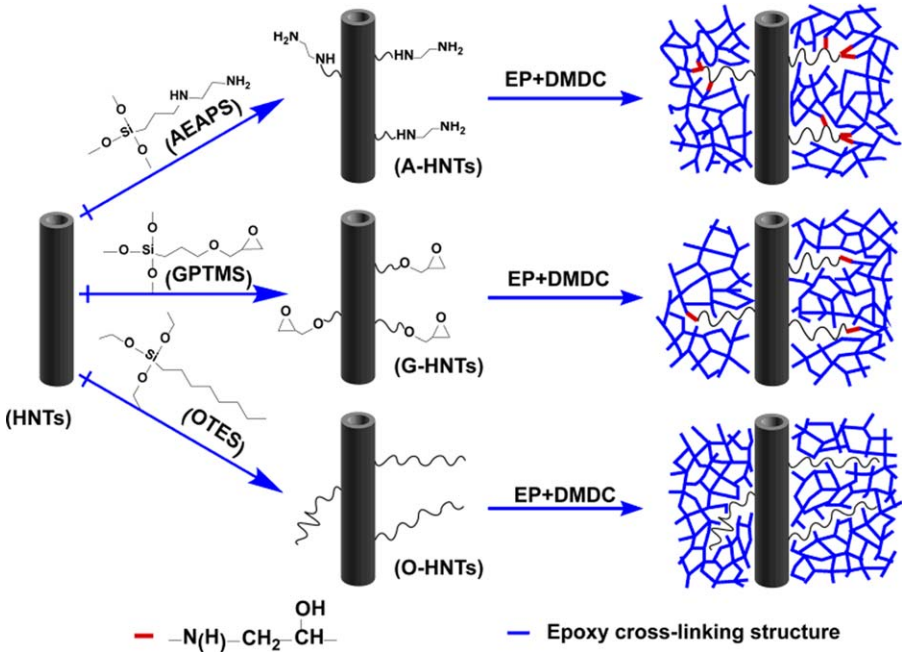

Figure 1. Schematic illustration of the silanization of HNTs and preparation of nanocomposites containing modified HNTs. [Color figure can be viewed in the online issue, which is available at wileyonlinelibrary.com.]

of epoxy nanocomposites containing PPA intercalated HNTs showed good improvement.[23] On the other hand, the PA and CTAC modified HNTs exhibited limited enhancement on the toughness or strength of epoxy.[21] Recently, increasing attentions have been paid on the modification of HNTs by using silane coupling agents with epoxy or amino groups. For example, Liu *et al.*[25] reported that a small amount of (3-glycidoxypropyl)-trimethoxysilane modified HNTs could increase the flexural strength and modulus of epoxy. However, a decreased flexural strength was observed when the amount of HNTs reached 12 wt %. Deng *et al.*[21] modified HNTs using 3-(2-aminoethyl)-aminopropyl- trimethoxysilane. The toughness and strength of epoxy nanocomposites containing modified HNTs was decreased compared with unmodified HNTs. More recently, direct tip sonication method was found as a powerful tool to obtain homogeneously dispersed HNTs, and the impact strength of the corresponding epoxy nanocomposites was improved. However, only slight variations of tensile strength and modulus were observed.[26] To date, a systematic study of the effect of different silanes has not been undertaken.

Sodium hydroxide is an activation agent to increase the density of hydroxyl groups on HNTs surfaces,[22] and the activated HNTs had higher reactivity with silanes.[26] In the present study, we selected three types of silanes containing epoxy, amino, or alkyl end groups to modify the HNTs. Subsequently, the obtained HNTs with different functionality were added to epoxy resin through solution mixing and two steps of tip-sonication process. The effects of silane functionalization of HNTs on the impact strength, tensile properties, and thermal properties of epoxy nanocomposites were studied. It is interesting to observe that the strength, toughness, and thermal properties of epoxy are improved simultaneously by silane modified HNTs.

EXPERIMENTAL

Materials

Epoxy resin EPON828 was purchased from Momentive Corporation. 3,3′-dimethyl-4,4′-diamino- dicyclohexylmethane (DMDC) which purchased from BASF Corporation was used as the curing agent. HNTs were collected from Hubei province China and purified through repeated sedimentation processes to remove possible impurities. The organosilanes used for the modification of HNTs were: 3-(2-aminoethyl)-aminopropyltrimethoxysilane (AEAPS, 98%), (3-glycidyloxypropyl)-trimethoxysilane (GPTMS, 98%), and octyltriethoxysilane (OTES, 98%). All of them were purchased from Sinopharm Chemical Reagent. And used as received.

Preparation of Silanized HNTs

HNTs suspension in alkaline solution (1*M*, NaOH) was stirred at room temperature for 24 h. The resultant HNTs were centrifugal separated and washed with distilled water for several times till the pH value of the suspension closed to 7. The activated HNTs were then dried overnight at 100°C before silanization treatments.

The silane modified HNTs were prepared following the procedure previously reported.[27] Two g of HNTs and 100 g of dry toluene were magnetic stirring for 30 min in a three-neck flask, followed by ultrasonically stirred for 30 min. About 0.4 g of silane was added drop wisely into the suspension. The mixture was refluxed at 120°C for 12 h and the resultant mixture was filtered, washed, and dried overnight at 110°C. The samples functionalized with AEAPS, GPTMS, and OTES were designated as A-HNTs, G-HNTs, and O-HNTs, respectively.

Preparation of Epoxy Nanocomposites

An ultrasonic assisted solution-evaporation method was used to achieve good dispersion of HNTs. The effectiveness of this

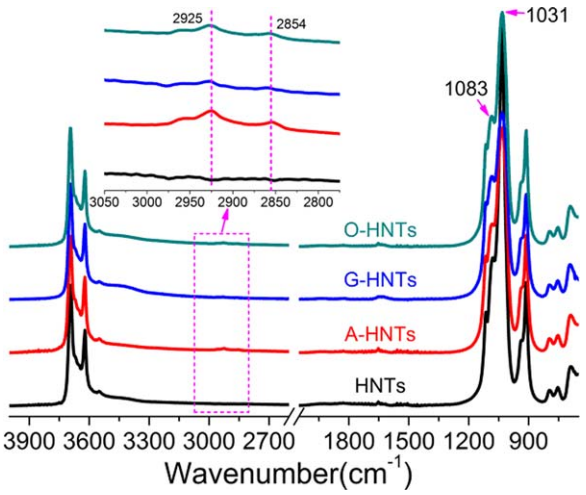

Figure 2. FTIR spectra of HNTs and modified HNTs samples with different silanes. [Color figure can be viewed in the online issue, which is available at wileyonlinelibrary.com.]

method has been proved in epoxy nanocomposites containing graphene,[28] Al_2O_3,[29] and CNTs.[30] Epoxy nanocomposites containing 2.5 wt % and 5 wt % HNTs were manufactured according to the following process. HNTs were firstly dispersed in chloroform, using a Scientz sonicator (250 W). The epoxy resin was then added to the HNTs suspension with tip sonication for 45 min in an ice bath. The solvent was evaporated during continually stirring for 12 h at 75°C. After solvent evaporation, DMDC (weight ratio: epoxy/DMDC = 100/33) was added into the mixture. After 30 min degassing, the mixture was poured into a stainless steel mold, and then cured at 80°C for 2 h and further cured at 150°C for another 2 h. A schematic was shown in Figure 1 illustrating the process of silane modification.

Characterization

Fourier transform infrared (FTIR) spectroscopy was conducted using a Nicolet 6700 FTIR spectrometer. Spectra were recorded in the range of 650–4000 cm^{-1}. Thirty two scans were averaged at a resolution of 4 cm^{-1}.

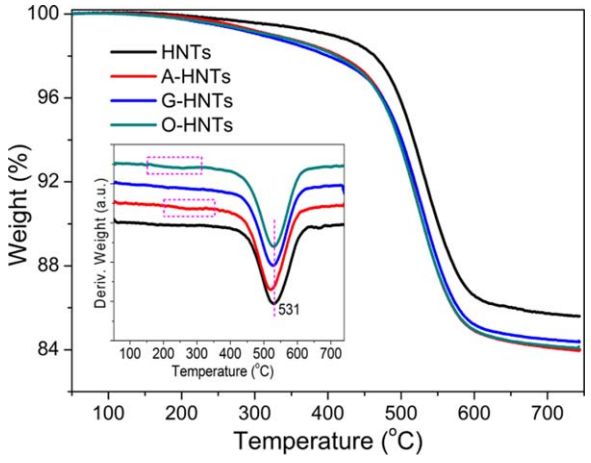

Figure 3. TG and DTG curves (inset) of the unmodified and silane modified HNTs. [Color figure can be viewed in the online issue, which is available at wileyonlinelibrary.com.]

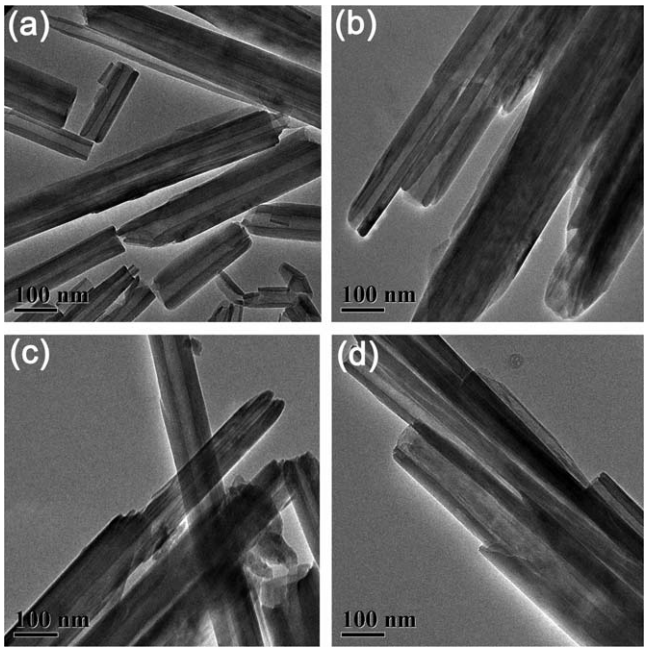

Figure 4. TEM images of (a) HNTs, (b) A-HNTs, (c) G-HNTs, and (d) O-HNTs.

Thermogravimetric analysis (TGA) of HNTs and nanocomposites was performed on a Pyris1 TGA instruments. Approximately 2–3 mg samples were heated with a heating rate of 10°C/min in a platinum crucible from 50°C to 750°C under high purity N_2 atmosphere.

TEM images were obtained by JEM-2200FS electron microscope performed at an acceleration voltage of 200 kV. The powder specimens were prepared by dropping the ethanol suspension of

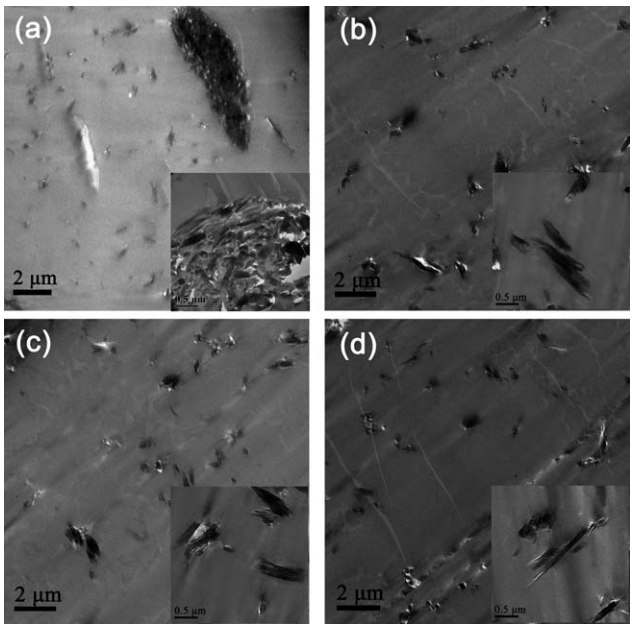

Figure 5. TEM images of epoxy nanocomposites containing 5 wt % of HNTs: (a) HNTs, (b) A-HNTs, (c) G-HNTs, and (d) O-HNTs. Insets show higher magnification images.

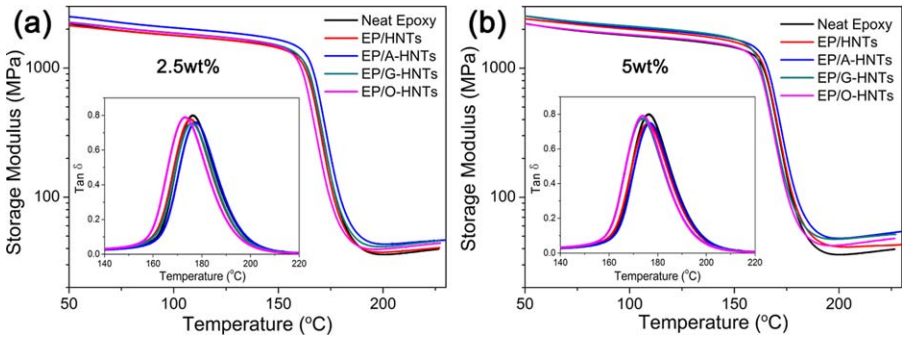

Figure 6. Storage modulus and loss factor (tan δ, insets) of the epoxy nanocomposites containing (a) 2.5 wt % and (b) 5 wt % HNTs. [Color figure can be viewed in the online issue, which is available at wileyonlinelibrary.com.]

sample onto a Formvar-coated copper grid. Ultrathin sections (about 100 nm) of nanocomposites were prepared by an ultramicrotome (Leica EMUC6) with a diamond knife.

Dynamic mechanical analysis (DMA) was conducted on a TA instrument (Q800) in single cantilever mode. Rectangular samples with a dimension of 30×12×2.5 mm were used. Temperature scans were measured at 1 Hz from 30°C to 230°C at a constant heating rate of 3°C/min.

Notched Charpy impact tests were performed according to ISO 179 on an impact tester (XJC-250) with pendulum energy of 0.5 J and a span of 60.0 mm. A 45° V shaped notch (2 mm) was made at the middle of the impact specimen (80× 10×4 mm) by a motorized notching machine (RAY-RAN) with a notch-tip radius of 0.25 mm. For each formula, at least seven specimens were tested.

Tensile properties of epoxy nanocomposites were determined according to ISO 527-1 on a universal testing machine (Instron 3365). Dumbbell shape samples (Type IBA of ISO 527-1) were first tested at a crosshead speed of 0.3 mm/min to acquired modulus, and then performed at 2.0 mm/min. At least five specimens were tested for each formula.

Scanning electron microscope (JEOL 6700) was used to study the morphology of the fracture samples and HNTs dispersion in epoxy matrix. The fracture surfaces of the cured epoxy/HNTs nanocomposites were coated with platinum to avoid charging.

Table I. Storage Modulus G' (50°C and 200°C) and tan δ Peak Temperature of Epoxy/HNTs Nanocomposites Obtained from Dynamic Mechanical Analysis

Samples	G' at 50°C (MPa)	G' at 200°C (MPa)	Tg (°C)	Tan δ peak height
Neat epoxy	2210	36	176	0.80
EP/HNTs(2.5%)	2125	37	175	0.78
EP/A-HNTs(2.5%)	2502	43	175	0.76
EP/G-HNTs(2.5%)	2258	41	176	0.75
EP/O-HNTs(2.5%)	2403	40	173	0.79
EP/HNTs(5%)	2531	41	176	0.75
EP/A-HNTs(5%)	2528	48	177	0.75
EP/G-HNTs(5%)	2528	47	174	0.77
EP/O-HNTs(5%)	2202	42	174	0.79

RESULTS AND DISCUSSION

Characterization of Modified HNTs

Fourier Transform Infrared Spectroscopy. Pristine HNTs and modified HNTs were characterized by FTIR to confirm the silane moieties on the surface of HNTs. As shown in Figure 2, characteristic peaks were observed, such as inner-surface AlO-H stretching band at 3694 cm^{-1}, inner AlO-H stretching band at 3621 cm^{-1}, O-H deformation vibration of water at 1650 cm^{-1}, and O-H deformation of inner-surface and inner Al-OH at 940 and 913 cm^{-1}. The bands at 1083 and 1031 cm^{-1} are related to the in plane Si-O stretching, and at 1114 cm^{-1} are related to the apical Si-O stretching. The symmetric stretching of Si-O-Si at 796 cm^{-1} and the perpendicular stretching of Si-O-Al at 754 cm^{-1} can also be observed.[31]

Compared with the pristine HNTs, all the three modified HNTs showed new peaks at 2925 and 2854 cm^{-1}, which can be assigned to the asymmetric and symmetric stretching vibration of aliphatic -CH_2. The efficiency of HNTs modification decreased in the order of G-HNTs< O-HNTs< A-HNTs. In addition, the peak ratio of 1083 to 1031 cm^{-1}in the three modified HNTs samples was higher than that of unmodified HNTs. The intensified peak at around 1083cm^{-1} was ascribed

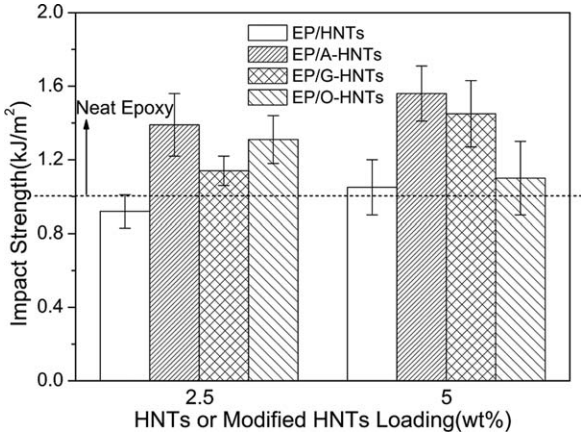

Figure 7. The impact strength of the epoxy/HNTs nanocomposites.

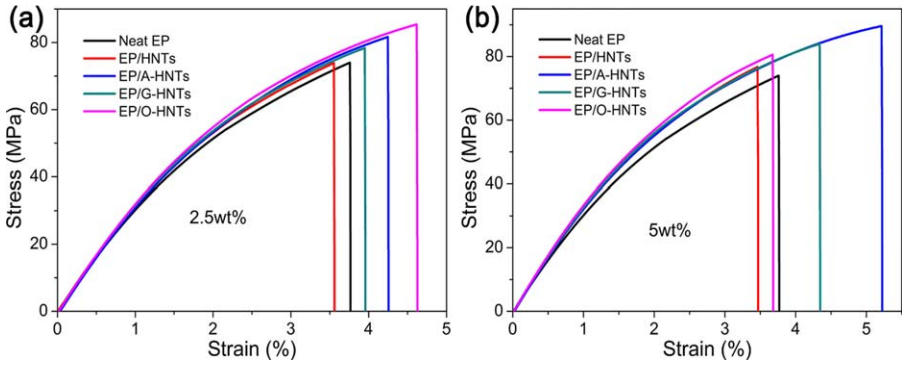

Figure 8. Stress–strain curves of nanocomposites filled with (a) 2.5 wt % and (b) 5 wt % of HNTs. [Color figure can be viewed in the online issue, which is available at wileyonlinelibrary.com.]

to the in plane Si-O stretching because of the surface grafted silane agents.[32]

TGA Analysis. Figure 3 shows the residual weight curves during heating of the HNTs. From the TG curves, the grafted amount of all the three modified HNTs is around 2%. Assuming a monolayer of silane formed on the HNTs surface, the percent of surface area covered by the silane is estimated to ~86%. The A-HNTs possessed the highest weight loss, which was in accordance with the FTIR result. The major weight loss at around 531°C was attributed to the dehydroxylation of the residual structural Al-OH groups. In addition, A-HNTs and O-HNTs had an apparent weight loss from 150°C to 350°C, corresponding to the decomposition of the hydrogen-bonded and chemical-bonded silane on the surface of HNTs.[31]

Transmission Electron Microscopy. The morphology of the unmodified and silane modified HNTs were further investigated by TEM. As shown in Figure 4, all the HNTs displayed hollow tubular microstructure. The external diameter of HNTs ranged from 50 to 150 nm, and their lumen diameter varied from 10 to 50 nm. Compared with unmodified HNTs, silane modified HNTs showed nearly no difference in morphology. As reported in the literature,[31] the intercaltion of silane into the interlayer of HNTs did not occur, and only the surface and ends of HNTs were available for grafting. However, it is still hard to detect the grafting layer morphologically.

Structure and Properties of EP/HNTs Nanocomposites

Morphology. Figure 5 displays the TEM images of the cured epoxy composites filled with 5 wt % HNTs. Micro-sized aggregates of HNTs are observed in EP/HNTs [Figure 5(a)]. A closer examination showed that the aggregates contained loosely packed HNTs with many small voids. Figure 5(b–d) show the TEM micrographs of the epoxy composites containing silane modified HNTs. Only bundles of several HNTs and individual HNTs can be detected. Similar morphology has been observed in epoxy/sepiolite nanocomposites, especially for the nanocomposites containing GPTMS-modified sepiolite.[33] Surface functionalization of HNTs with AEAPS or GPTMS could lead to a better interaction between the HNTs and epoxy matrix, thus improved the dispersion of HNTs in nanocomposites. Although the alkyl chains on the surface of O-HNTs had relatively weak interaction with epoxy, the hydrophobic groups of O-HNTs could also weaken the interaction between nanotubes. Therefore, the weak interaction makes O-HNTs possessing the relatively better dispersion than unmodified HNTs in epoxy resin.

Dynamic Mechanical Analysis. The DMA curves presented in Figure 6 provide information regarding the storage modulus and relaxation behavior of materials. The storage modulus at 50°C and 200°C, the glass transition temperature, and the height of the glass transition peak are summarized in Table I. When the HNTs loading was 2.5 wt % [Figure 6(a)], only the EP/A-HNTs showed obvious modulus enhancement (13.2%) at

Table II. Tensile Properties of the Epoxy/HNTs Nanocomposites

Samples	Tensile strength (MPa)	Young's modulus (GPa)	Elongation at break (%)	Toughness (MJ/m^3)[a]
Neat epoxy	74.0 ± 1.6	3.00 ± 0.13	3.76 ± 0.37	1.69 ± 0.17
EP/HNTs(2.5%)	73.2 ± 0.8	3.09 ± 0.16	3.56 ± 0.43	1.60 ± 0.23
EP/A-HNTs(2.5%)	79.7 ± 2.0	3.18 ± 0.06	4.26 ± 0.45	2.15 ± 0.19
EP/G-HNTs(2.5%)	78.4 ± 2.9	3.15 ± 0.12	3.96 ± 0.27	1.92 ± 0.31
EP/O-HNTs(2.5%)	84.8 ± 2.4	3.15 ± 0.09	4.62 ± 0.39	2.51 ± 0.34
EP/HNTs(5%)	76.7 ± 3.4	3.20 ± 0.16	3.47 ± 0.32	1.59 ± 0.22
EP/A-HNTs(5%)	89.6 ± 3.3	3.34 ± 0.23	5.22 ± 0.48	3.05 ± 0.13
EP/G-HNTs(5%)	84.0 ± 2.1	3.27 ± 0.22	4.35 ± 0.24	2.30 ± 0.40
EP/O-HNTs(5%)	80.6 ± 3.5	3.31 ± 0.14	3.69 ± 0.34	1.81 ± 0.21

[a] Toughness was calculated from the area under the stress–strain curve.

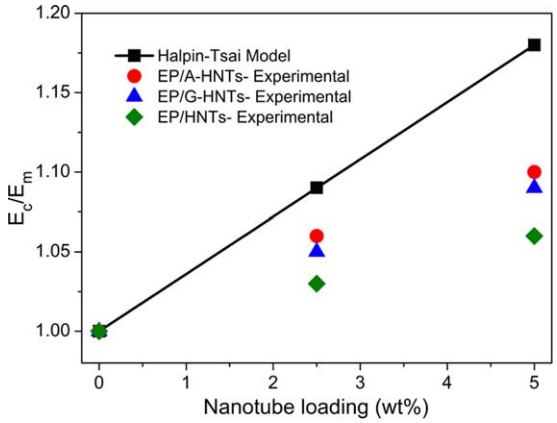

Figure 9. The normalized Young's modulus of epoxy/HNTs nanocomposites and Halpin-Tsai prediction. [Color figure can be viewed in the online issue, which is available at wileyonlinelibrary.com.]

50°C. On the other hand, all the nanocomposites display higher storage modulus compared with neat epoxy at 200°C. The T_g of EP/O-HNTs was slightly lower than that of the neat epoxy, while all other composites exhibited similar T_g as the neat epoxy. When the HNTs loading was 5 wt %, the storage modulus of nanocomposites was higher than that of neat epoxy both below or above T_g except EP/O-HNTs. Compared with EP/A-HNTs, EP/O-HNTs and EP/G-HNTs have slightly decreased T_g.

T_g characterizes the chain segmental mobility which is determined mainly by the chemical structure and also is related to the interfacial interaction for nanocomposites. The T_g variation of epoxy nanocomposites is proposed to be a result of two competitive factors: the enhanced interaction and the decreased cross-linking density of epoxy.[17,34] Compared with the unmodified HNTs, the enhanced interaction between the A-HNTs and epoxy restricted the motion of chain segments. For the EP/O-HNTs composites, the effect of the flexibility of OTES and the possible decrease in cross-linking density may lead to the lower T_g. The height of tan δ peak can reflect the interfacial load transfer in the nanocomposites. Smaller values usually resulted from more efficient stress transfer.[22,35,36] As presented in Figure 6, the EP/A-HNTs and EP/G-HNTs exhibit lower tan δ peak, indicating more effective load transfer.

Impact Strength. Figure 7 shows the impact strength of epoxy/HNTs nanocomposites. The impact strength of the neat epoxy was around 1 kJ/m^2 and was plotted as a dash line in Figure 7. By adding unmodified HNTs, the impact strength of nanocomposite was lower than neat epoxy when the HNTs loading was 2.5 wt %, and was comparable to neat epoxy when the HNTs loading was 5 wt %. It can be observed that nanocomposites containing modified HNTs had 25–50% increase in impact strength than those containing unmodified HNTs. The enhancing effect of HNTs depended on the functional groups of silane.

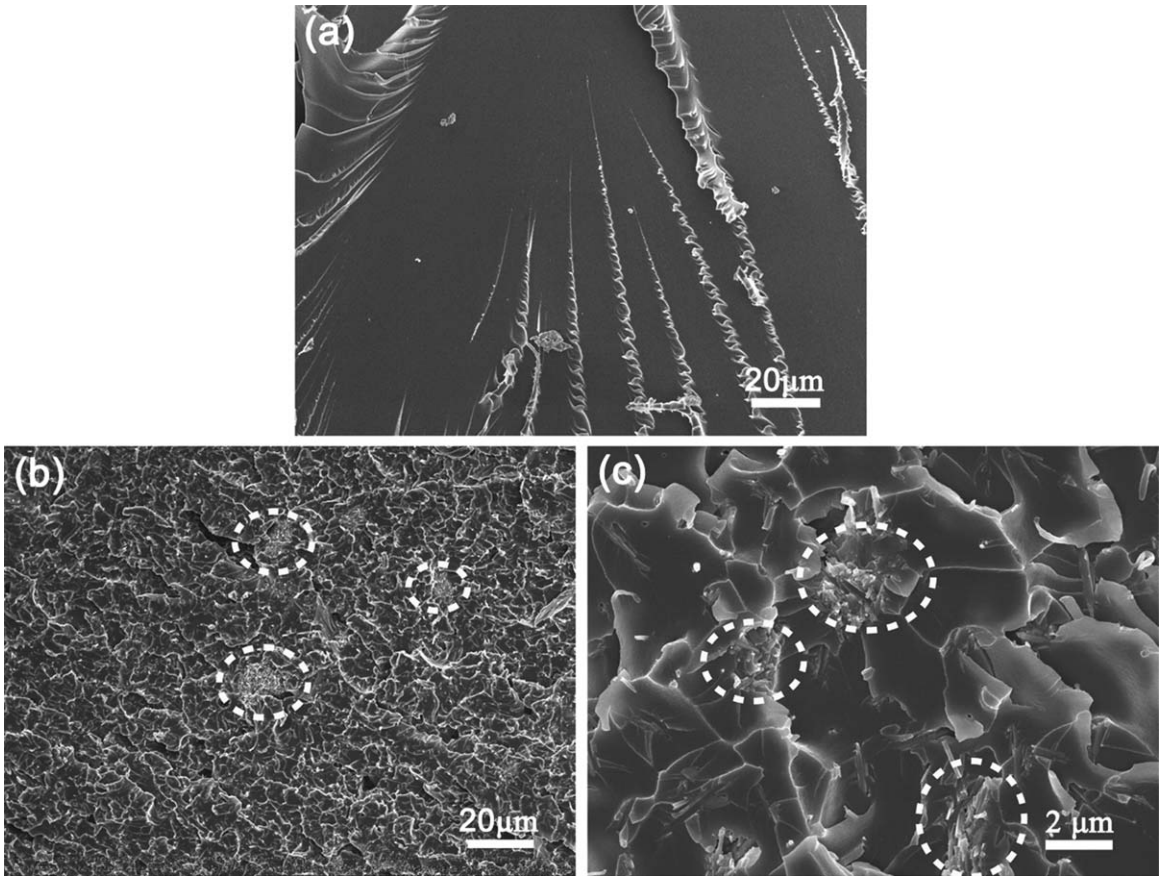

Figure 10. SEM images of the fracture surface of (a) neat epoxy and (b,c) composites filled with 5 wt % unmodified HNTs. Dotted circles show the aggregates of HNTs.

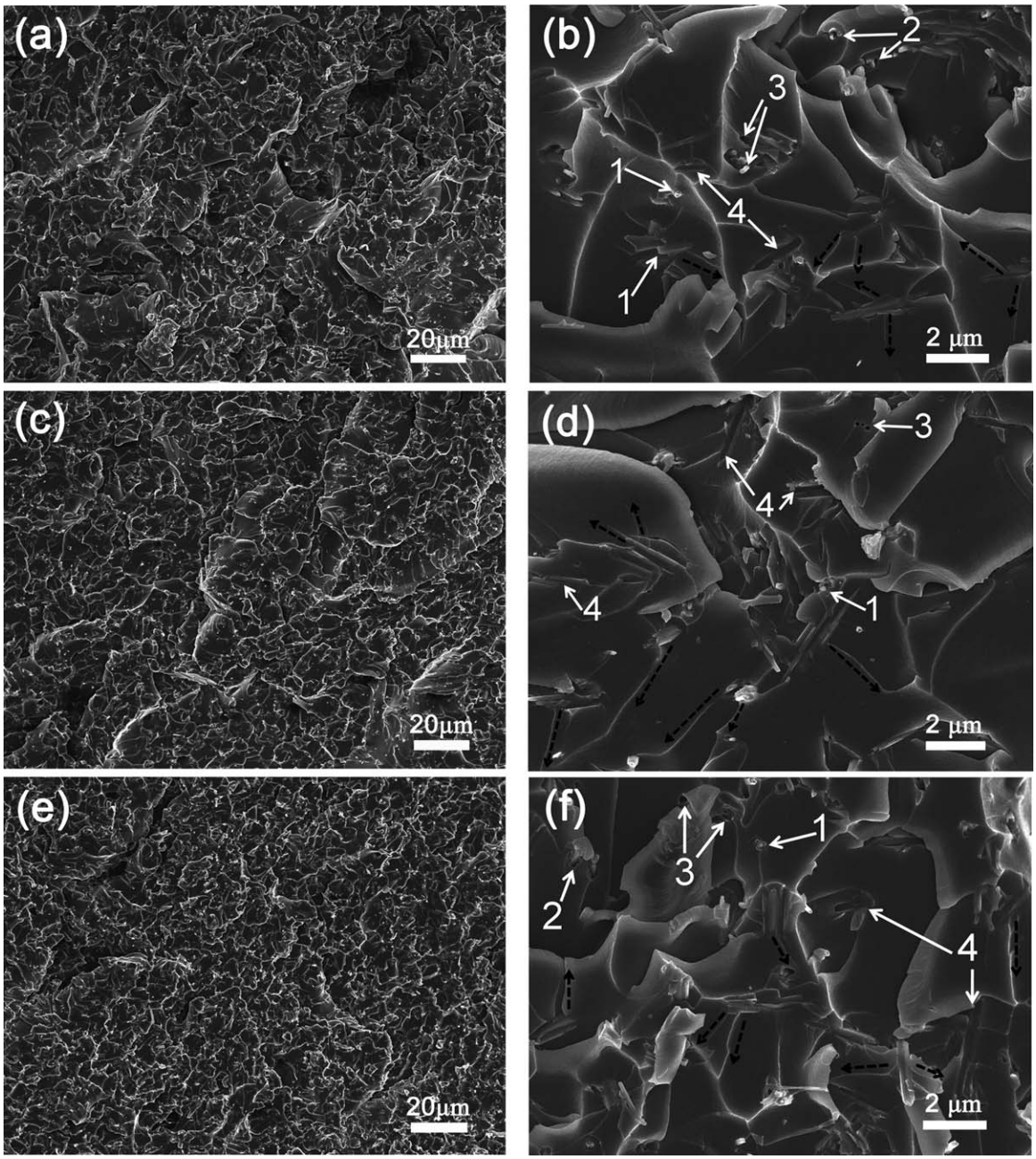

Figure 11. SEM images of the tensile fracture surface of epoxy nanocomposites with 5 wt % HNTs: (a,b) A-HNTs (c,d) G-HNTs (e,f) O-HNTs. The bifurcation paths and tails are indicated by dashed black arrows. The white arrows and markers: *1*- nanotube rupture, *2*- voids growth (small gap between debonded HNTs and the surrounding epoxy), *3*- holes after pulling-out of nanotube aligned perpendicular to the crack front, *4*- grooves after pulling-out of nanotube aligned parallel to the crack front.

The EP/A-HNTs exhibited the highest impact strength in comparison to EP/G-HNTs and EP/O-HNTs. The EP/G-HNTs showed 14% enhancement in impact strength when the G-HNTs loading was 2.5 wt %, while a 45% increase of impact strength was observed when the G-HNTs loading increased to 5 wt %. The EP/O-HNTs containing 2.5 wt % had a moderate enhancement (31%) of impact strength. However, a decrease of impact strength was observed when the HNTs loading were 5 wt %. The A-HNTs contributed to the highest increase in impact strength (56%, 5 wt % A-HNTs). The results showed that the epoxy or amino groups of modified HNTs could enhance the interfacial adhesion between the matrix and HNTs. And the homogeneous dispersion of the modified HNTs may be beneficial for enhancing the toughness.[37]

Tensile Properties. Figure 8 displays the stress–strain curves of epoxy nanocomposites containing different types of HNTs. The corresponding mechanical parameters are summarized in Table II. The incorporation of 2.5 wt % unmodified HNTs slightly decreased the tensile strength and elongation at break [Figure

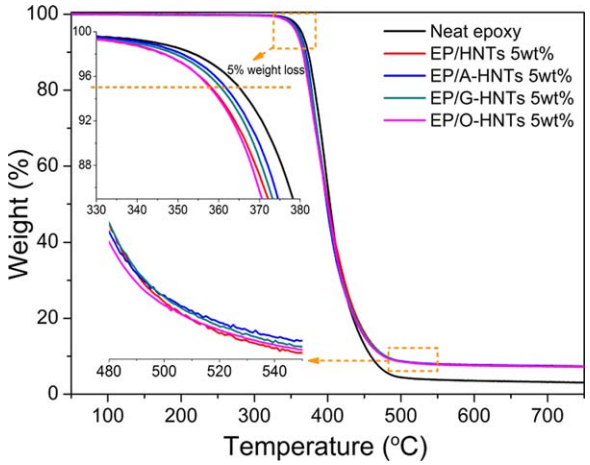

Figure 12. TGA curves of nanocomposites containing 5 wt % HNTs. The insets are magnified views of the regions of interest. [Color figure can be viewed in the online issue, which is available at wileyonlinelibrary.com.]

8(a)]. The tensile strength and elongation at break increased in epoxy nanocomposites containing modified HNTs, though the modulus remained largely unchanged within error. The improvement of elongation at break suggested that the modified HNTs could improve the energy absorption and deform together with the matrix without slippage.[38] The flexible siloxane chains interacted with the matrix during curing may contribute to this improvement.[35] As shown in Figure 5, modified HNTs had better dispersion in the epoxy matrix, which was beneficial for the improvement of strength and modulus.[39] The area under stress–strain curves can characterize the toughness of nanocomposites, which is also listed in Table II. The A-HNTs were found to have a more pronounced effect on toughness, resulting in 27% and 80% increases compared with neat epoxy (2.5 and 5 wt % loading, respectively). It is interesting to observe that 2.5 wt % O-HNTs exhibited the highest tensile strength and elongation at break, while 5 wt % O-HNTs showed the lowest tensile properties compared with other modified HNTs. The reason is still unclear.

To further evaluate the efficiency of the load transfer, the experimental tensile modulus was compared with the prediction of Halpin-Tsai model. For nanotube reinforced composites, the modified Halpin-Tsai model was usually applied[40]:

$$\frac{E_c}{E_m}=\frac{3}{8}\times\frac{1+2(l_{NT}/d_{NT})\eta_L V_{NT}}{1-\eta_L V_{NT}}+\frac{5}{8}\times\frac{1+2\eta_T V_{NT}}{1-\eta_T V_{NT}}$$

$$\eta_L=\frac{E_{NT}/E_m-1}{E_{NT}/E_m+2(l_{NT}/d_{NT})}$$

$$\eta_T=\frac{E_{NT}/E_m-1}{E_{NT}/E_m+2}$$

where E_c, E_m, and E_{NT} are the modulus of nanocomposites, epoxy matrix (3 GPa, from Table II), and nanotube (130 GPa[41]), respectively; l_{NT} is the length; and d_{NT} is the outer diameter of the nanotubes. The value of l_{NT}/d_{NT} is 8, calculated from the TEM images. The nanotube volume fraction V_{NT} was calculated from the weight fraction (2.5 or 5 wt %), density of HNTs[4] (2.5 g/cm^3) and EP (1.2 g/cm^3, tested according to ASTM D792). The experimental and predicted Young's modulus against HNTs contents are shown in Figure 9. The experimental modulus of EP/A-HNTs is the closest to the model prediction. This result further suggests that A-HNTs have the most efficient stress transfer. The larger deviation in modulus for EP/HNTs could be induced by the presence of larger aggregates.

Morphology of the Fracture Surface. Figure 10 displays the typical SEM images of the tensile fracture surfaces of the neat epoxy and nanocomposites containing 5 wt % unmodified HNTs. The neat epoxy shows smooth surface with jagged river-line markings, which is characteristic for brittle failure [Figure 10(a)]. As to EP/HNTs, nonplanar rough surfaces were observed [Figure 10(b)]. Micro-sized aggregates of HNTs can be observed in Figure 10(b,c), which would initiate crack extension during tensile test.[22]

Figure 11 presents the SEM images of the nanocomposites containing 5 wt % modified HNTs. The fracture surfaces of EP/A-HNTs and EP/G-HNTs were rougher than that of EP/O-HNTs. The increased roughness of fracture surface indicated that modified HNTs could enhance the ductility and plastic deformation of epoxy matrix.[12,42] This result is in good agreement with the increase of elongation at break.

Crack deflection is usually recognized as an effective toughening mechanism for nanoparticles with high aspect ratios.[43] In the vicinity of individual HNTs or bundled HNTs, crack deflection introduces sliding or tearing loading, thus increasing the energy consumed for crack propagation. After crack initiation, the bridged nanotubes at the crack front could be completely pulled out or fractured, depending on the interfacial adhesion between the nanotube and epoxy matrix. Small holes and protruding segment of A-HNTs shown in Figure 11(b) (marked as "3") indicated that A-HNTs were pulled out of the epoxy matrix, and small white dots were fractured A-HNTs (marked "1"). It has been reported that CNTs-based nanocomposites showed similar phenomena,[44,45] with a relatively higher percentage of nanotube fracture. Plastic void growth (marked "2") was also observed as the small gaps between partial embedded HNTs and the surrounding epoxy. Meanwhile, A-HNTs could resist crack propagation through characteristic crack tip bifurcation (dash black arrows),[45] which often lead to increased toughness. Pulling-out of A-HNTs that were aligned parallel to the crack plane (marked "4") was occurred in the fracture surface.

The nanotubes debonding, fracture, void growth around nanotubes, and crack deflection and crack pinning, all could contribute to the toughening effect of modified HNTs. Almost all those energy absorbing processes for toughening can be found in EP/O-HNTs. However, O-HNTs had relatively lower percentage of nanotube fracture (marked "1") and void growth (marked "2").

Thermal Stability. The thermal stability of epoxy nanocomposites was studied by TGA, as shown in Figure 12. The TGA curves of epoxy nanocomposites containing HNTs showed similar decomposition profiles as the neat epoxy. The addition of A-HNTs or G-HNTs enhanced the initial decomposition temperature (5 wt % weight loss) in comparison to the pristine HNTs. The A-HNTs showed the highest thermal stability among all the nanocomposites. The increased interaction between A-HNTs and epoxy matrix may contribute to the retardation of the permeation of volatile gas

out of the nanocomposites during thermal decomposition.[46] From the initial decomposition temperature and char yield, the EP/O-HNTs composite showed the lowest thermal stability.

CONCLUSIONS

In this work, surface functionalization of HNTs with three types of silane was performed and verified through FTIR and TGA. In comparison with pristine HNTs, the silane modified HNTs exhibited improved dispersion and interfacial interaction in the epoxy matrix. The mechanical properties of composites can be controlled by the interfacial interaction between the functional group of silane and the matrix. The epoxy nanocomposites with modified HNTs using AEAPS and GPTMS exhibited improved strength and toughness without sacrificing the elongation at break. The EP/A-HNTs showed the best mechanical performance. TGA results demonstrated that epoxy containing A-HNTs and G-HNTs exhibited higher thermal decomposition resistance compared with unmodified HNTs.

ACKNOWLEDGMENTS

The authors wish to thank the financial support of Hong Kong, Macao and Taiwan Science and Technology Cooperation Project (2012DFH50110) Ministry of Science and Technology of China, the Strategic Priority Research Program (XDA01020304) of the Chinese Academy of Sciences. J.S.W. is grateful for the support from the Innovation and Technology Commission (ITC), Hong Kong SAR (Project No.: GHP/039/12). G.M.L. acknowledges the support from the Youth Innovation Promotion Association of the Chinese Academy of Sciences (2015026).

REFERENCES

1. Du, M.; Guo, B.; Jia, D. *Eur. Polym. J.* **2006**, *42*, 1362.
2. Du, M.; Guo, B.; Liu, M.; Jia, D. *Polym. J.* **2007**, *39*, 208.
3. Abdullayev, E.; Lvov, Y. *J. Mater. Chem. B.* **2013**, *1*, 2894.
4. Liu, M.; Jia, Z.; Jia, D.; Zhou, C. *Prog. Polym. Sci.* **2014**, *39*, 1498.
5. Sun, P.; Liu, G.; Lv, D.; Dong, X.; Wu, J.; Wang, D. *Sci. China. Technol. Sci.* **2015**, *45*, 602.
6. Deng, S.; Zhang, J.; Ye, L.; Wu, J. *Polymer* **2008**, *49*, 5119.
7. Lin, Y.; Ng, K. M.; Chan, C. M.; Sun, G.; Wu, J. *J. Colloid. Interface Sci.* **2011**, *358*, 423.
8. Handge, U. A.; Hedicke, H. K.; Altstädt, V. *Polymer* **2010**, *51*, 2690.
9. Prashantha, K; Lacrampe, M.; Krawczak, P. *Express Polym. Lett.* **2011**, *5*, 295.
10. Lvov, Y.; Abdullayev, E. *Prog. Polym. Sci.* **2013**, *38*, 1690.
11. Liu, M.; Guo, B.; Du, M.; Jia, D. *Polym. J.* **2008**, *40*, 1087.
12. Albdiry, M. T.; Yousif, B. F. *Mater. Design* **2014**, *57*, 279.
13. Riza, E. A.; Kaygusuz, I.; Kaynak, C. *Polym. Compos.* **2014**, *35*, 1350.
14. Guo, B.; Zou, Q.; Lei, Y.; Jia, D. *Polym. J.* **2009**, *41*, 835.
15. Pasbakhsh, P.; Ismail, H.; Fauzi, M.; Bakar, A. A. *Appl. Clay Sci.* **2010**, *48*, 405.
16. Domun, N.; Hadavinia, H.; Zhang, T.; Sainsbury, T.; Liaghat, G. H.; Vahid, S. *Nanoscale* **2015**, *7*, 10294.
17. Ye, Y.; Chen, H.; Wu, J.; Ye, L. *Polymer* **2007**, *48*, 6426.
18. Vahedi, V.; Pasbakhsh, P.; Chai, S. P. *Mater. Design* **2015**, *68*, 42.
19. Alamri, H.; Low, I. M. *Polym. Compos.* **2012**, *33*, 589.
20. Alamri, H.; Low, I. M. *Mater. Design* **2012**, *42*, 214.
21. Deng, S.; Zhang, J.; Ye, L. *Compos. Sci. Technol.* **2009**, *69*, 2497.
22. Zeng, S.; Reyes, C.; Liu, J.; Rodgers, P. A.; Wentworth, S. H.; Sun, L. *Polymer* **2014**, *55*, 6519.
23. Tang, Y.; Deng, S.; Ye, L.; Yang, C.; Yuan, Q.; Zhang, J.; Zhao, C. *Compos. Part A* **2011**, *42*, 345.
24. Tang, Y.; Ye, L.; Deng, S.; Yang, C.; Yuan, W. *Mater. Design* **2012**, *42*, 471.
25. Liu, M.; Guo, B.; Du, M.; Lei, Y.; Jia, D. *J. Polym. Res.* **2008**, *15*, 205.
26. Vahedi, V.; Pasbakhsh, P. *Polym. Test.* **2014**, *39*, 101.
27. Sun, P.; Liu, G.; Lv, D.; Dong, X.; Wu, J.; Wang, D. *RSC Adv.* **2015**, *5*, 52916.
28. Wang, X.; Xing, W.; Zhang, P.; Song, L.; Yang, H.; Hu, Y. *Compos. Sci. Technol.* **2012**, *72*, 737.
29. Yu, J.; Huang, X.; Wang, L.; Peng, P.; Wu, C.; Wu, X.; Jiang, P. *Polym. Chem.* **2011**, *2*, 1380.
30. Kathi, J.; Rhee, K. Y.; Lee, J. H. *Compos. Part A* **2009**, *40*, 800.
31. Yuan, P.; Southon, P. D.; Liu, Z.; Green, M. E. R.; Hook, J. M.; Antill, S. J.; Kepert, C. J. *J. Phys. Chem. C.* **2008**, *112*, 15742.
32. Li, C.; Wang, J.; Luo, X.; Ding, S. *J. Colloid Interface Sci.* **2014**, *420*, 1.
33. Franchini, E.; Galy, J.; Gérard, J. F. *J. Colloid Interface Sci.* **2009**, *329*, 38.
34. Yu, W.; Fu, J.; Dong, X.; Chen, L.; Jia, H.; Shi, L. *ACS Appl. Mater. Interfaces* **2013**, *5*, 8897.
35. Vennerberg, D.; Rueger, Z.; Kessler, M. R. *Polymer* **2014**, *55*, 1854.
36. Tang, G.; Jiang, Z.; Li, X.; Zhang, H.; Yu, Z. *Chin. J. Polym. Sci.* **2014**, *32*, 975.
37. Niu, X.; Huo, L.; Cai, C.; Guo, J.; Zhou, H. *Ind. Eng. Chem. Res.* **2014**, *53*, 16359.
38. Ma, P.; Zheng, Q.; Mäder, E.; Kim, J. K. *Polymer* **2012**, *53*, 6081.
39. Pavlidou, S.; Papaspyrides, C. D. *Prog. Polym. Sci.* **2008**, *33*, 1119.
40. Qian, D.; Dickey, E. C.; Andrews, R.; Rantell, T. *Appl. Phys. Lett.* **2000**, *76*, 2868.
41. Lu, D.; Chen, H.; Wu, J.; Chan, C. M. *J. Nanosci. Nanotechnol.* **2011**, *11*, 7789.
42. Zhu, J.; Wei, S.; Ryu, J.; Budhathoki, M.; Liang, G.; Guo, Z. *J. Mater. Chem.* **2010**, *20*, 4937.
43. Faber, K. T.; Evans, A. G. *Acta Metall.* **1983**, *31*, 565.
44. Tang, L.; Zhang, H.; Wu, X.; Zhang, Z. *Polymer* **2011**, *52*, 2070.
45. Shtein, M.; Nadiv, R.; Lachman, N.; Daniel Wagner, H.; Regev, O. *Compos. Sci. Technol.* **2013**, *87*, 157.
46. Tseng, C. H.; Wang, C. C.; Chen, C. Y. *Chem. Mater.* **2007**, *19*, 308.